Downregulation of chemokine (C-C motif) ligand 5 induced by a novel 8-hydroxyquinoline derivative (91b1) suppresses tumor invasiveness in esophageal carcinoma

JOHNNY CHEUK-ON TANG[1,2], DESSY CHAN[2], PO-YEE CHUNG[2], YIJIANG LIU[3], ALFRED KING-YIN LAM[4], SIMON LAW[5], WOLIN HUANG[1], ALBERT SUN-CHI CHAN[6], KIM-HUNG LAM[2] and YUANYUAN ZHOU[2,7]

[1]Jean-Marie Lehn Laboratory, Guangzhou Huashang College, Guangzhou, Guangdong 511300, P.R. China; [2]State Key Laboratory of Chemical Biology and Drug Discovery, The Hong Kong Polytechnic University, Hong Kong, SAR 999077, P.R. China; [3]School of Biological Sciences, Nanyang Technological University, Singapore 639798, Republic of Singapore; [4]Griffith Medical School, Griffith University, Gold Coast, QLD 4222, Australia; [5]Department of Surgery, Li Ka Shing Faculty of Medicine, The University of Hong Kong, Pokfulam, Hong Kong, SAR 999077, P.R. China; [6]President Office, Guangzhou Huashang College, Guangzhou, Guangzhou 511300, P.R. China; [7]Department of Life Science and Engineering, Foshan University, Foshan, Guangdong 528000, P.R. China

Received April 5, 2024; Accepted August 6, 2024

DOI: 10.3892/ijmm.2024.5435

Abstract. Esophageal squamous cell carcinoma (ESCC) is a particularly aggressive form of cancer with high mortality. In the present study, a novel 8-hydroxyquinoline derivative (91b1) was investigated for its anticancer activities in ESCC along with its associated mechanisms. The *in vitro* cytotoxic effect of 91b1 were evaluated across five ESCC cell lines using MTS assay, with cisplatin serving as a comparative standard. Changes in gene expression profile were identified by cDNA microarray and further validated by qualitative PCR and immunostaining. Additionally, protein levels of the most notably downregulated target in archival ESCC samples were also studied. 91b1 demonstrated comparable anticancer effect with cisplatin. Notably, chemokine ligand 5 (*Ccl5*) was identified as the most substantially downregulated gene, with its suppression at both mRNA and protein expression in ESCC cells, exhibiting a dose-dependent manner. The recombinant human protein of CCL5 enhanced the invasion of ESCC cells using the Transwell assay. The upregulation of CCL5 protein was also detected in 50% of ESCC cell lines. CCL5 was also overexpressed in 76.9% of ESCC specimens. The overall results indicated that 91b1 could effectively induce anticancer effect on ESCC cells through downregulating CCL5 expression with suppression of tumor invasion. Overall, these findings suggested that 91b1 effectively inhibited ESCC cell proliferation and tumor invasion by downregulating CCL5 expression, highlighting its potential as a therapeutic agent for ESCC treatment.

Correspondence to: Dr Johnny Cheuk-On Tang, Jean-Marie Lehn Laboratory, Guangzhou Huashang College, 1 Huashang Road, Licheng Street, Zengcheng, Guangzhou, Guangdong 511300, P.R. China
E-mail: jtang@graduate.hku.hk

Dr Yuanyuan Zhou, Department of Life Science and Engineering, Foshan University, 33 Guangyun Road, Shishan, Nanhai, Foshan, Guangdong 528000, P.R. China
E-mail: zhouyy@fosu.edu.cn

Key words: esophageal squamous cell carcinoma, chemokine (C-C motif) ligand 5, quinoline derivatives

Introduction

Patients with esophageal squamous cell carcinoma (ESCC) usually have poor prognosis and high mortality rate due to the aggressiveness of the tumors (1). In 2020, it was responsible for >604,100 new cases and ~544,076 mortalities worldwide (2). Currently, adjuvant chemotherapy plays a central role in the treatment of esophageal cancer as one third of patients are found with metastatic disease at the time of diagnosis. Chemotherapy comprising cisplatin (CDDP) results in response rates in esophageal carcinoma ≥40%. However, emergence of chemoresistance to chemotherapeutic drugs and severe side effect with toxicity lead to suboptimal survival rate (3,4), underscoring the urgent need for novel and more effective chemotherapeutic agents.

Chemokine ligand 5 (CCL5), part of the CC chemokine family, is recognized by CCR1, CCR3, and CCR5 receptors (5). Predominantly expressed in T cells, macrophages and cancer cells, CCL5 modulates the expression of the surface receptors, the phenotypes of cancer cells, or the tumor microenvironments reshaping to enhance cancer progression and metastases (6-9). Although its involvement in liver (10), prostate (11) and pancreatic cancer (12) is well documented, its role in ESCC and its underlaying mechanisms remains to be elucidated. According to the pan-cancer

analysis and Immunohistochemical (IHC) verification in ESCC cell lines and patients' samples in the present study, CCL5 was usually highly expressed in cancer cells or tumor tissue, suggesting its potential as a therapeutic target to ESCC.

Natural products, particularly quinoline and its derivatives, are well known for their diverse pharmacological applications (13-18). For example, 4-hydroxy-6-methoxy-quinoline-2-carboxylic acid (Fig. 1A), which can be isolated from *Ephedra pachyclada ssp*. Sinaica, has been traditionally used to treating microbial, inflammation, allergy and cardiovascular diseases (13). Another notable quinoline derivative, quinine, from the bark of cinchona trees, is renowned for its efficacy in malaria treatment. In addition, propyl quinoline, which is one of the active ingredients in exudates of bark of *Galipea. longiflora* (*Rutaceae*) trees, is recognized for its effectiveness against leishmaniasis (14). Among different quinoline-based compounds, 8-hydroxyquinoline derivatives, which can be extracted from the root of a plant *Commelina. Diffusa* (15), stand out due to their broad range of pharmacological efficacies (16-18). As prominent *in vitro* and *in vivo* anticancer effects of 8-hydroxylquinoline derivatives were also reported in our previous studies (19-23), a series of novel quinoline derivatives were then synthesized by our group (23-26). A total of 27 compounds were examined for anti-cancer activities against cancer cell lines of hepatocellular carcinoma (Hep3B), lung carcinoma (A549), and esophageal squamous cell carcinoma (HKESC-1, HKESC-4, and KYSE150). Compound 91b1 (its original name in our published patent is compound 2b) exhibited marked anti-cancer activity (25). Additionally, other compounds with anti-cancer effect were also studied and some of them have been reported. For example, quinoline compound 83b inhibits cancer growth in esophageal squamous cell carcinoma by downregulating COX-2 and PGE2 (22). The cytotoxic potential 6 quinoline derivatives were examined *in vitro* and *in vivo* (19). 2-formyl-8-hydroxy-qinolinium chloride was prepared and its anti-cancer activity was evaluated *in vitro* and *in vivo* (20).

Subsequent molecular docking analysis on the synthesized 8-hydroxylquinoline derivatives was performed to identity the potential protein targets involved in their anticancer actions. Recently a novel quinoline derivative 91b1 (5,7-dibromo-1,2,3,4-tetrahydro-2-methylquinolin-8-ol) (Fig. 1B) was reported which suppressed the tumor growth both *in vitro* and *in vivo* through downregulating the expression of Lumican (27).

In the present study, the biological actions of the most differentially expressed genes (DEGs) caused by 91b1 were investigated based on the microarray analysis for gene expression profiling. The protein expression levels of the most DEGs were also examined on archival samples to underscore the therapeutic relevance of 91b1 in the treatment of ESCC. The findings highlighted that the 91b1-induced cytotoxicity was associated with the downregulation of chemokine CCL5. Taken together with the overexpression of CCL5 being a common event in the ESCC patient samples, the overall results emphasized the potential of 91b1 as a promising candidate for the treatment of ESCC.

Materials and methods

Bioinformatics analysis. Pan-cancer analysis of *Ccl5* was conducted by Tumor Immune Estimation Resource (TIMER) 2.0 (28). *Ccl5* was entered into the TIMER 2.0 web interface (http://timer.cistrome.org/), 'Gene_DE module' was applied to study the differential expression between tumor and adjacent normal tissues across all TCGA tumors. Distribution of gene expression are displayed using box plots. The gene expression profiling of *Ccl5* influence was obtained from GEO datasets GSE105042 (https://www.ncbi.nlm.nih.gov/geo/query/acc.cgi?acc=GSE105042). Then two wild type macrophages and two *Ccl5* knock out macrophages was retrieved from a mouse dataset using the GPL21273 HiSeq X Ten platform (Illumina, Inc.). The original gene expression profiles were analyzed to identify the upregulated or downregulated DEGs in *Ccl5* knock out samples, respectively. The criteria for a DEG were |log2FC|>1 and adjusted P-value <0.05. Gene Ontology (GO) enrichment analysis and Kyoto Encyclopedia or Genes and Genomes (KEGG) pathway analysis were performed using the R package cluster Profiler (v. 4.0.5; https://www.R-project.org) with identified DEGs (29). GO enrichment analysis and KEGG pathway analysis were performed with the thresholds of a P-value <0.05.

The Search Tool for the Retrieval of Interacting Genes/Proteins (STRING) database (https://string-db.org/) was used to construct the PPI network (30). DEGs were mapped to a STRING list to perform a search for multiple proteins and obtain a PPI network with interaction scores >0.4. Cytoscape (v. 3.9.0) was used to visualize the results from the PPI network and perform module analysis (31). Module analysis was performed using the molecular complex detection (MCODE) plugin on the Cytoscape (v. 3.9.0) platform. The parameters set to identify enriched functional modules were as follows: Degree Cutoff=2, Node Score Cutoff=0.2, K-Core=2 and Maximum. Depth=100. Modules with the MCODE score ≥4 were identified as significant modules.

Preparation of Compound 91b1 (5,7-dibromo-1,2,3,4-tetrahydro-2-methylquinolin-8-ol). Compound 91b1 (Fig. 1B) was prepared by addition of Br_2 into commercially available 8-hydroxy-2-methylquinolin-8-ol (MilliporeSigma) in MeOH, followed by asymmetric hydrogenation under optimal reaction condition as previously described (23). The structure of 91b1 has been physically characterized using 1H- and 13C-NMR and liquid chromatography mass spectrometry (LC-MS) as previously reported (22). Dimethyl sulfoxide (DMSO) was used to dissolve 91b1 for the *in vitro* biological assays as described below.

Cell lines. Esophageal squamous cell carcinoma (ESCC) cell lines of Japanese origin KYSE150, KYSE450, KYSE30 and KYSE510 (32) were purchased from Leibniz-Institut DSMZ-Deutsche Sammlung von Mikroorganismen und Zellkulturen GmbH. ESCC cell lines of Hong Kong origin SLMT-1 (33) and HKESC-4 (34) were kindly provided by Professor Gopesh Srivastava in the Department of Pathology, The University of Hong Kong, China. Non-neoplastic esophageal epithelial cell line NE-3 (35) (immortalized by the induction of genes E6 E7 of human papillomavirus type 18)

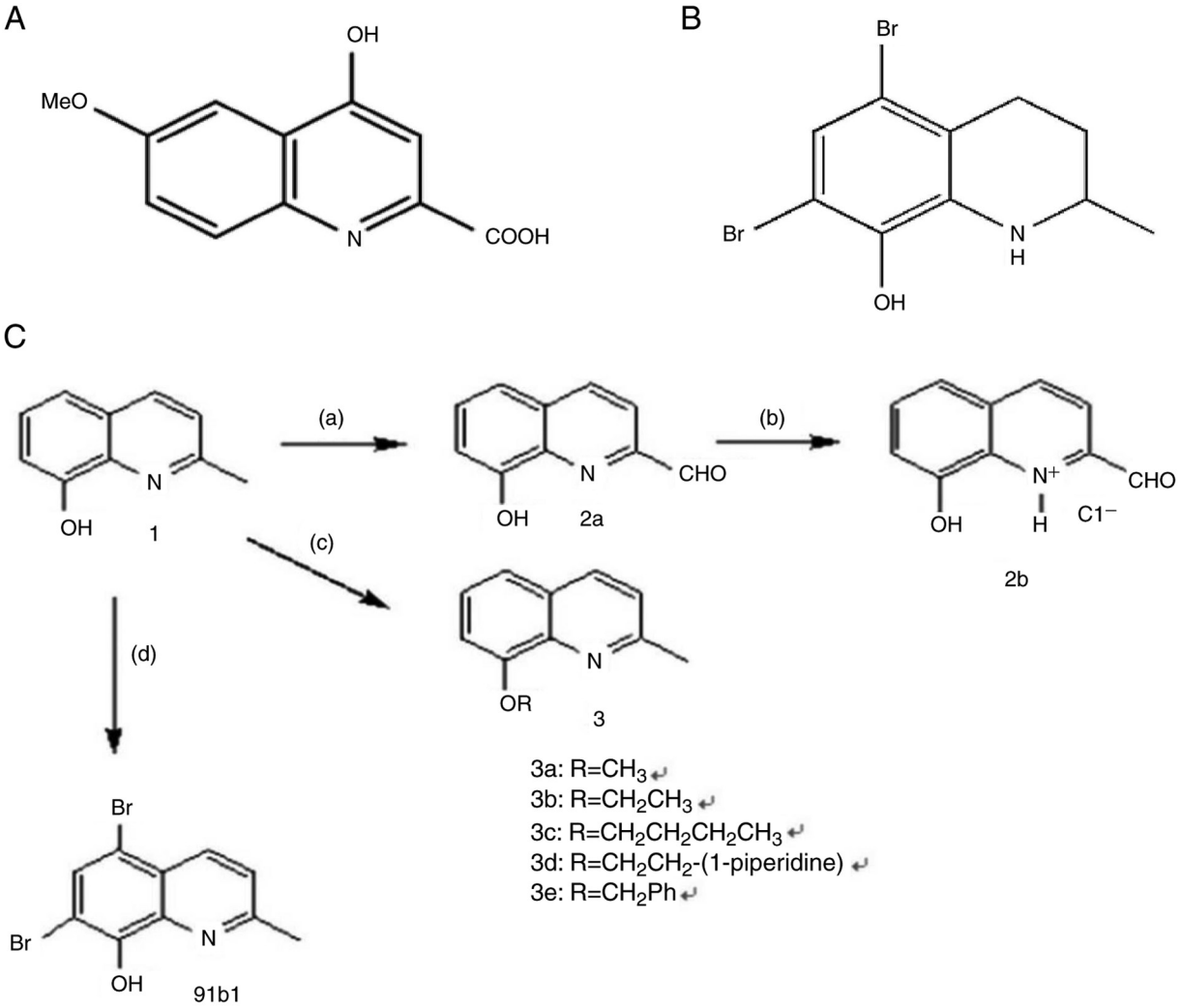

Figure 1. Structure of quinoline derivatives. (A) 4-hydroxy-6-methoxyquinoline-2-carboxylic acid. (B) 5,7-dibromo-1,2,3,4-tetrahydro-2-methylquinolin-8-ol (91b1). (C) The synthesis of quinoline derivatives. Reagents: (a) SeO_2, dioxane/H_2O, reflux; (b) HCl, (c) RX (X=Cl or Br), (d) Br_2.

was kindly provided by Professor George S.W. Tsao in the Department of Anatomy, The University of Hong Kong, China. Non-neoplastic embryonic cell line 293 (36) was purchased from the American Type Culture Collection (ATCC). The culture medium for KYSE30, KYSE150, KYSE450, and KYSE510 was 45% RPMI with 45% F-12 and 10% FBS; that for SLMT-1, HKESC4, and 293 was 90% MEMα with 10% FBS; and that for NE3 was KSFM with complementary supplements. All the cells were cultured in media supplemented with 100 units/ml penicillin G and 100 μg/ml streptomycin and all cells were maintained in a humidified atmosphere of 95% air and 5% CO_2 at 37˚C. The cultures were passaged at preconfluent densities of ~80% using a solution of 0.25% trypsin (Invitrogen; Thermo Fisher Scientific, Inc.). Cells were washed briefly with phosphate-buffered saline (PBS), treated with 0.25% trypsin, and harvested by centrifugation (300 x g for 5 min) at room temperature for subculturing.

ESCC patient specimens. Paraffin-embedded specimens containing 26 cancer tissues and 15 non-neoplastic tissues were collected after esophagectomy, with the consent of patients, at the Department of Surgery, Queen Mary Hospital, Hong Kong between January 1990 and December 2001 and the ethics approval for working on the specimens was obtained from the Hong Kong Polytechnic University (approval no. HSEARS20171213007). All the specimens were collected from patients who had received no prior treatment directed to the primary ESCC. The age of the patients ranged from 45 to 77 years old, with a median of 65, comprising 23 males and 3 females. Oral informed consent was obtained in from all patients. The authors confirm that all methods were carried out in accordance with relevant guidelines and regulations. The clinical and histological information of ESCC patient specimens were reported by a pathologist (AKY Lam).

[3-(4,5-dimethylthiazol-2-yl)-5-(3-carboxymethoxyphenyl)-2-(4-sulfophenyl)-2H-tetrazolium] (MTS) cytotoxicity assay. The cytotoxic effect of 91b1 and CDDP on the ESCC cell lines and non-neoplastic cell lines was examined by CellTiter-96-AQueous One Solution Cell Proliferation Assay (Promega Corporation) as previously described and expressed as the MTS_{50} values (27). Each assay was performed in triplicate.

cDNA microarray analysis. Total RNA was extracted from $2x10^8$ cells of KYSE150 treated with 91b1 at 9.5 μg/ml (based

on the MTS_{50} value of 91b1 on KYSE150 with the signal of MTS cytotoxicity decreased by 50%) and DMSO (0.05%; MilliporeSigma) for 48 h using RNeasy Mini kit (Qiagen, Inc.). The cDNA microarray analysis and the associated quality control using Human Genome U133 Plus 2.0 arrays (Affymetrix; Thermo Fisher Scientific, Inc.) were performed at the Centre for Genomic Sciences of the University of Hong Kong according to the manufacturer's protocol as previously described (4). The signals of the differentially expressed genes in 91b1-treated KYSE150 were compared with the DMSO-treated KYSE150 control.

Reverse transcription-quantitative (RT-q) PCR. The total RNA of non-neoplastic cells, ESCC parental cells and 91b1-treated ESCC cells was extracted using RNeasy Mini kit (Qiagen, Inc.) as previously described (4). cDNA was synthesized from total RNA using the GoScript Reverse Transcription System (Promega Corporation) according to manufacturer's instruction. The expression level of *Ccl5* in the tested cells was determined by qPCR analysis using Go Taq qPCR Master Mix (Promega Corporation) and Thermo Scientific PikoReal Real-Time PCR System (Thermo Fisher Scientific, Inc.) according to manufacturer's protocol. The synthesized cDNA (4 μl) was mixed with 10 μl of 2X qPCR Mastermix (Promega Corporation), 2 μl of 2 μM forward and reverse primers of either target gene or reference gene (β-Actin was applied as reference gene), and 12 μl of RNase free water to get a total volume of 20 μl in a PCR tube. All 20 μl of sample mixtures were transferred into the wells of PikoReal 96-well strips (n=3). qPCR reactions were carried out by PikoReal Real-Time PCR System (Thermo Fisher Scientific, Inc.). The thermocycling conditions were: Polymerase activation at 95˚C for 2 min, then followed by 40 cycles of denaturation at 95˚C for 15 sec, annealing and primer extension at 60˚C for 1 min, then melt curve data were identified by gradually increasing temperature from 60-95˚C until the fluorescent signal dropped to zero. Cq (cycle of quantification) of each sample was determined and recorded by the program PikoReal Software 2.0 (Thermo Fisher Scientific, Inc.). cDNA (~2 μg) produced by reverse transcription from the RNA was amplified using a specific *Ccl5* and β-Actin gene primer pairs (IDT). Primers for *Ccl5* were 5'-CGTGCCCACATCAAGGAG-3' (forward) and 5'-GGACAAGAGCAAGCAGAAA-3' (reverse). Primers for β-Actin were 5'-ACCTTCTACAATGAGCTGCG-3' (forward) and 5'-CCTGGATAGCAACGTACATGG-3' (reverse). Relative *Ccl5* expression was determined by comparing with vehicle DMSO (0.05%) control, after being normalized with expression of β-Actin. For all the qPCR reactions, the relative expression of target genes in different samples were calculated and compared by using the $2^{-\Delta\Delta Cq}$ method. The expression level of target genes was normalized by the reference gene β-actin. Each independent experiments is conducted three times.

The calculation of $2^{-\Delta\Delta Cq}$ method was (37):

$$\Delta Cq \text{ of target gene} = Cq \text{ of target gene} - Cq \text{ of reference gene}$$

$$\Delta\Delta Cq \text{ of target gene} = \Delta Cq \text{ of the target gene in treated group} - \Delta Cq \text{ of the target gene in control group}$$

Therefore, the fold change of gene expression level=$2^{-(\Delta\Delta Cq \text{ of target gene})}$

The expression level was regarded as overexpression if the fold change of gene expression level ratio

$$\left(\frac{\text{Target gene(tumor)/Reference gene(tumor)}}{\text{Target gene(non-tumor)/Reference gene(non-tumor)}}\right)$$

was larger than 1.2; a ratio between 0.8 and 1.2 was considered as no significant change, while a ratio smaller than 0.8 was considered as under expression of the target gene (38).

IHC staining. Paraffin-embedded cell-line blocks of KYSE150, KYSE510, KYSE450, KYSE520 KYSE30, HKESC-3 HKESC-4, SLMT-1, NE-3, DMSO-treated (0.05%, 48 h) and 91b1-treated (6.5, 9.5 and 21 μg/ml 91b1) for 48 h KYSE150 cells were prepared from ~$5x10^6$ cells of each respective cell line with formalin-fixation (37% formalin and 15% methanol at room temperature for 48 h). Flowing fixation, tissues were rinsed under running water for 3 h. Then the tissues underwent a grade dehydration process starting with 50% ethanol for 2 h, followed by 70% ethanol for 2 h, 80% ethanol overnight, 90 and 95% ethanol for 2 h each, and concluding twice in 100% ethanol for 2 h each time. Subsequently, the samples were placed in a mixture of ethanol:xylene (1:1) for 30 min and cleared in xylene for 30 min twice before being prepared for embedding in paraffin wax at 60˚C twice for 1 h each time. An automated embedding system was employed to encapsulate the tissues in paraffin. Dewaxed paraffin sections (8 μm) of cell-line blocks and samples from patients with ESCC were immunostained using the streptavidin-biotin-peroxidase complex method. As pretreatment, microwave-based antigen retrieval was be performed in 10 mM citrate buffer (pH 6.0). CCL5 mouse monoclonal antibody (1 mg/ml; Abnova) was applied at dilution of 1:100 for overnight incubation at 4˚C. Images of stained samples were captured under an inverted optical microscope (CKX41; Olympus Corporation) at magnification, x400 and four fields of images of stained sections were examined for the percentage of positively stained cells in cytoplasm by ImageJ (v 1.54; National Institutes of Health). Immunostaining results of ESCC cell line were compared with that of non-tumor cell line NE-3. Immunohistochemical staining images of stained sections were examined and graded according to the percentage of positively stained neoplastic cells as previously described (4).

Enzyme-linked immuno-sorbent assay (ELISA). Protein expression levels of CCL5 in cells were measured using RANTES (CCL5) Human SimpleStep ELISA kit (Abcam; cat. no. ab174446) according to the manufacturer's instructions. Cells receiving no treatment, DMSO-treatment (0.05%) or 91b1-treatment in the concentration of 6.5, 9.5 and 21 μg/ml (with reference to the MTS_{50} value) were collected by cell scrapper after 48 h. Total protein concentration of each sample was determined using a Micro BCA Protein Assay kit (Thermo Fisher Scientific, Inc.) according to manufacturer's manual for normalization.

Transwell Matrigel invasion assay. The invasion ability of ESCC cells was evaluated using chambers with Matrigel-coated membrane (8-μm pore size; BD Biocoat;

Corning, Inc.) in 24-well plate. The lower chamber was filled with RPMI 1640 medium (Gibco; Thermo Fisher Scientific, Inc.) containing 10% fetal bovine serum (FBS, Biosera) with recombinant human CCL5 protein (rhCCL5; Abnova) at concentration of 0, 50, 100 and 500 ng/ml. KYSE30 cells were cultured in 200 μl serum free RPMI 1640 medium in the upper chamber at a density of $2.5x10^5$ cells/ml. The same number of cells were cultured on an uncoated membrane (8-μm pore size) chamber as control. After 24 h, the uninvaded cells on the upper chamber were scraped off with a cotton swab. The transmembrane cells which migrated to the opposite side of the membrane were fixed in 100% methanol for 10 min and stained with 0.5% crystal violet solution (0.5 g crystal violet in 75 ml methanol and 25 ml ddH_2O) for 30 sec at room temperature after washing twice with phosphate buffered saline (PBS). The transmembrane cells were counted under microscope in five random fields at magnification of x100. The percentage of invasion was calculated as follows:

$$\% \text{ invasion} = \frac{\text{mean number of cell invading through matrigel coated membrane}}{\text{mean number of cells migrating through uncoated membrane}} \times 100$$

Wound-healing assay. A wound-healing assay was performed to evaluate cell migration and growth. KYSE150 cells (~$1x10^6$) were cultured in a 6-well plate at 37˚C with 5% CO_2 overnight to let the cells adhere and grow to 70-80% confluent monolayers. On the second day, the monolayer was gently scratched with a new 1 ml pipette tip across the center of the well to generate a wound area without changing the medium. After scratching, the well was gently washed twice with warm PBS buffer to remove detached cells, and the well was replenished with serum-starved medium or different concentrations of compound 91b. The cells were incubated at 37˚C with 5% CO_2 again and observed by microscope (Olympus CKX41; Olympus Corporation) at different time points (0, 12, and 24 h after scratching) for image capture. The number of cells invaded across the wound area was counted by ImageJ (v 1.54, National Institutes of Health).

Statistical analysis. The comparative ΔΔCq method was applied for relative quantification in qPCR analysis. Statistical significance of the differences among groups in MTS cytotoxicity assay, qPCR analysis, ELISA, Transwell Matrigel invasion assay data were compared by two-tailed t test or one-way analysis of variance (ANOVA) followed by Dunnett's Correction using GraphPad Prism 7 (Dotmatics). $P<0.05$ was considered to indicate a statistically significant difference.

Results

Bioinformatics analysis of the function of Ccl5 in cancers. According to the pan-cancer analysis in Fig. 2A, *Ccl5* was differentially expressed in several types of cancer, in which *Ccl5* was notably high expressed in breast invasive carcinoma, esophageal carcinoma, glioblastoma multiforme, head and neck squamous cell carcinoma, kidney renal clear cell carcinoma, kidney renal papillary cell carcinoma and metastasis skin cutaneous melanoma, suggesting the possible roles of *Ccl5* in tumorigenesis and tumor metastasis.

GO enrichment analysis results are in Fig. 2B. The most enriched GO molecular functions were identified as 'small GTPase mediated signal transduction', 'regulation of GTPase activity', 'lymphocyte differentiation', 'regulation of protein serine/threonine kinase activity', 'regulation of MAP kinase activity', 'cell-substrate adhesion', 'protein folding', 'wound healing', 'actin filament organization' and 'positive regulation of kinase activity'. KEGG pathway analysis results are in Fig. 2C, indicating that the DEGs were enriched in nine pathways, 'coronavirus disease', 'prion disease', 'human T-cell leukemia virus 1 infection', 'regulation of actin cytoskeleton', 'ribosome', 'lipid and atherosclerosis', 'non-alcoholic fatty liver disease', 'growth hormone synthesis, secretion and action', 'antigen processing and presentation' and 'viral myocarditis'.

A total of 1,579 interactions were obtained with interaction scores >0.4 using the STRING database. The PPI network was then constructed and presented with the Cytoscape (v. 3.9.0) platform (Fig. 2D). The top 10 hub genes included *Itgb2, Pik3cg, Pik3r1, Cbl, Pten, Syk, Pik3cb, Ptprc, Met* and *Inpp5d*. A total of four modules were obtained through MCODE analysis. The function of key proteins, such as PIK3, PTEN, and ATM were associated with metastases, IFNG, CD74, CD40, and CD3g were associated with immune response.

CCL5 is usually high expressed in ESCC cell lines and patient samples. Immunostaining was employed to detect the cytoplasmic protein expression level of CCL5 in eight ESCC cell lines and non-tumor esophageal cell line NE-3. Upregulation of CCL5 was detected in 7/8 (87.5%) ESCC cell lines (KYSE510, KYSE450, KYSE520, KYSE150, HKESC-3, HKESC-4 and SLMT-1) when compared with NE-3 (Fig. 3A and B). In addition, high expression level of CCL5 was also observed in 20/26 (76.9%) of ESCC tissues and only 6/15 (40%) of non-neoplastic esophageal tissues. ESCC expressing CCL5 protein in high level was more frequently observed than non-neoplastic esophageal mucosa ($P=0.018$). Immunohistochemical staining showed high expression and low expression of CCL5 in ESCC (Fig. 3C).

The effect of CCL5 on the invasion ability of KYSE30 was examined by Transwell Matrigel invasion assay. As shown in Fig. 3E, no transmembrane cells were detected in the invasion assay after 24 h without the addition of recombinant human CCL5 protein (rhCCL5). Increasing numbers of transmembrane cells were detected with increasing rhCCL5 concentration. The percentage of invasion increased with the concentration of rhCCL5 (Fig. 3G), suggesting that CCL5 enhanced the invasion ability of ESCC cells. Moreover, to evaluate the cell migration and growth properties affected by compound 91b1, wound healing analysis was performed on KYSE510 cell line. A wound gap was created by scratching, and healing progress was captured at different time points. Cancer cells were treated with low (5 μg/ml) or high (10 μg/ml) dose of compound 91b1 (Fig. 3D and F). After 12-h, or 24-h incubation, fewer cells of compound 91b1 treatment groups migrated into the scratched area than the control groups, indicating the reduction of cell migration of the cancer cells following 91b1 treatment.

Compound 91b1 downregulated the expression of Ccl5 in ESCC cells. cDNA microarray analysis was performed to study the changes of gene expression caused by compound 91b1 in cancer cells. Density plots (Fig. 4A) showed the

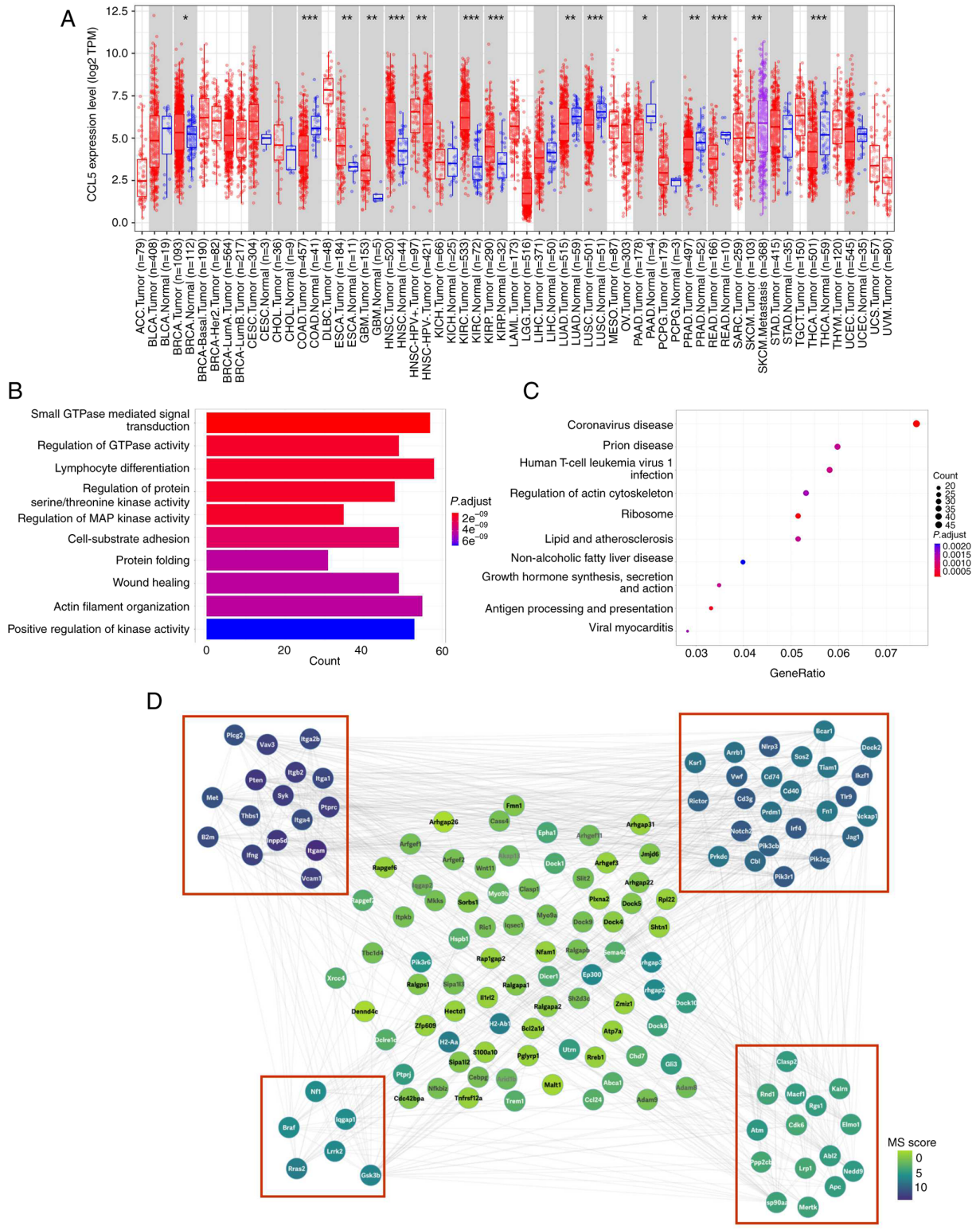

Figure 2. CCL5 plays a critical role in several types of cancers, and its related functions mainly enriched in metastasis and immunology. (A) Pan-cancer analysis of CCL5 by TIMER 2.0, upregulated or downregulated genes in the tumors were compared with normal tissues for each cancer type, as displayed in gray columns when normal data were available; red dots indicate tumor tissue, blue dots indicate normal tissue, purple dots indicate metastasis tumor tissue, *P<0.05; **P<0.01; ***P<0.001; (B) GO enrichment analysis; (C) KEGG pathway analysis; (D) PPI analysis. PPI network for all the overlapping DEGs was constructed and followed by module analysis using the MCODE plugin on the Cytoscape (v. 3.9.0) platform. Modules with a red border are significant modules. The size of circles reflects the degree of connectivity. CCL5, chemokine (C-C motif) ligand 5; PPI, protein-protein interaction; GO, Gene Ontology; KEGG, Kyoto Encyclopedia or Genes and Genomes; DEGs, differentially expressed genes.

different expression profile of KYSE150 cells treated with compound 91b1 compared with a blank control. The fold changes of normalized signal intensity of each gene obtained from the microarray analysis were evaluated. The five most downregulated genes were *Ccl5, Lumican, Ston1, Igfb5* and *Cp* while the five most upregulated genes were *C7orf57, Zbed2,*

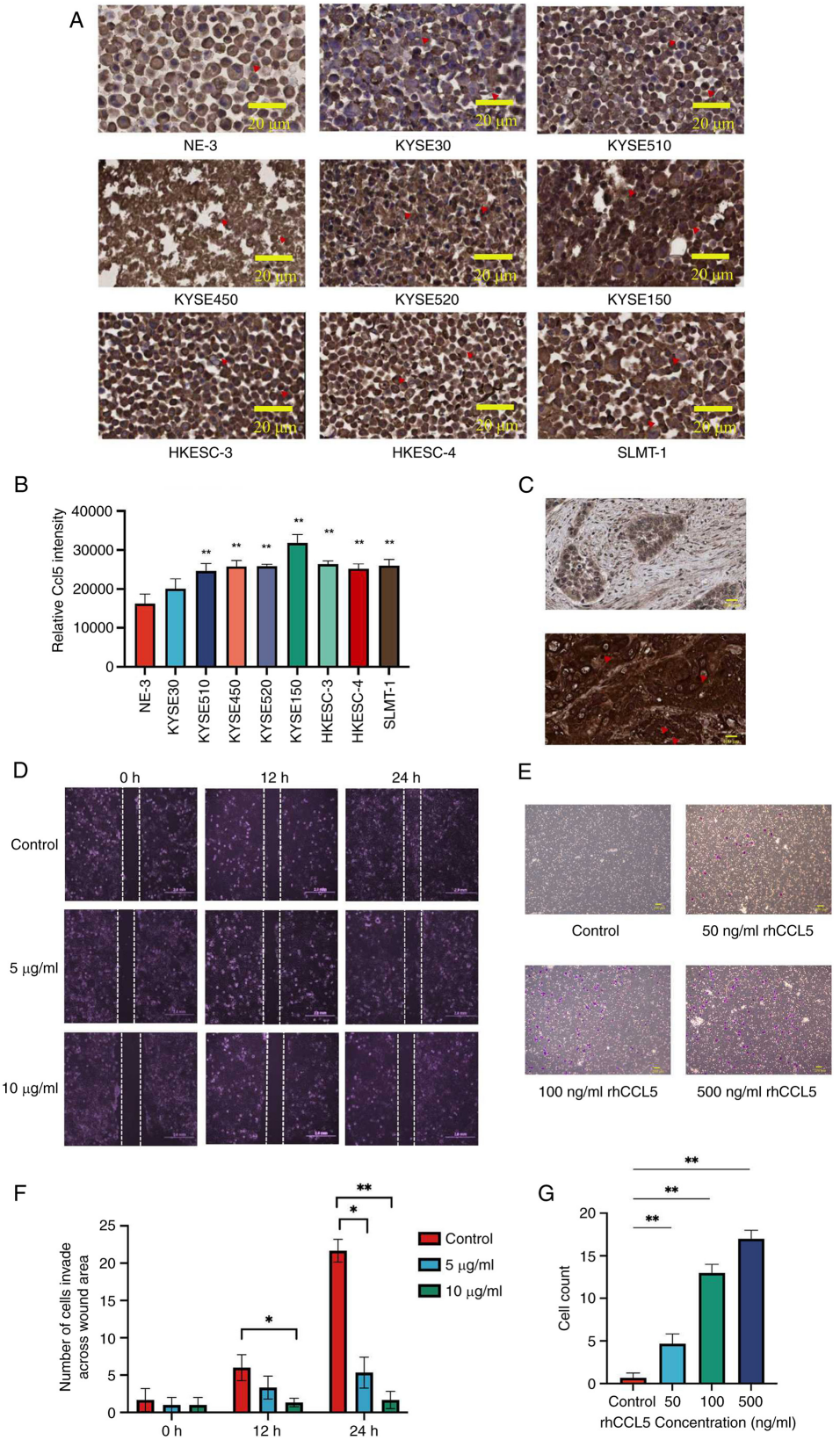

Figure 3. CCL5 is usually highly expressed in ESCC cell lines and patient samples, enhanced cancer cell invasion which can be suppressed by compound 91b1. (A) Immunohistochemical staining of CCL5 in eight ESCC cell lines, non-tumor cell line NE-3 with (B) quantitative analysis, Original magnification, x400; scale bar, 200 μm. (C) Representative images of immunohistochemical staining for CCL5 in ESCC specimens graded as low expression (upper photo) and high expression (lower photo), Original magnification, x400; scale bar, 200 μm. Red triangles represent IHC staining of CCL5 protein in cancer cells or specimens. (D) Images of wound healing progress of KYSE150 cells under 5 μg/ml or 10 μg/ml compound 91b1 at 0, 12 and 24 h respectively with average cell count invaded across the wound area, Original magnification, x100; scale bar, 2 mm (F); (E) Cell Invasion assay using Transwell Matrigel chamber with 0 ng/ml rhCCL5 (control), 50 ng/ml rhCCL5, 100 ng/ml rhCCL5, and 500 ng/ml rhCCL5. Transmembrane cells were stained by crystal violet, Original magnification, x200; scale bar, 200 μm; (G) Average invaded cell count of KYSE150 co-cultured with different concentrations of rhCCL5 (0, 50, 100, 500 ng/ml). The invaded cells were counted under a microscope in four random fields. *P<0.05; **P<0.01. CCL5, chemokine (C-C motif) ligand 5; ESCC, esophageal squamous cell carcinoma.

Table I. List of the five most down- and upregulated genes in KYSE150 cells treated with 91b1 (9.5 μg/ml) for 48 h compared with the vehicle control.

A, Genes downregulated in 91b1-treated KYSE150 cells		
Probe set ID	Gene name	Fold-change
1405_i_at	*Ccl5*, chemokine (C-C motif) ligand 5	-2.12
201744_s_at	LUM, *Lumican*	-2.07
213413_at	STON1, *Stonin* 1	-1.80
211959_at	*Igfbp5*, insulin-like growth factor binding protein 5	-1.79
1558034_s_at	*Cp*, ceruloplasmin	-1.79
B, Genes upregulated in 91b1-treated KYSE150cells		
1557636_a_at	*C7orf57*, chromosome 7 open reading frame 57	1.89
219836_at	*Zbed2*, zinc finger, BED-type containing 2	1.71
205830_at	*Clgn*, calmegin	1.66
210229_s_at	*Csf2*, colony stimulating factor 2	1.65
230748_at	*Slc16a6*, solute carrier family 16, member 6	1.58

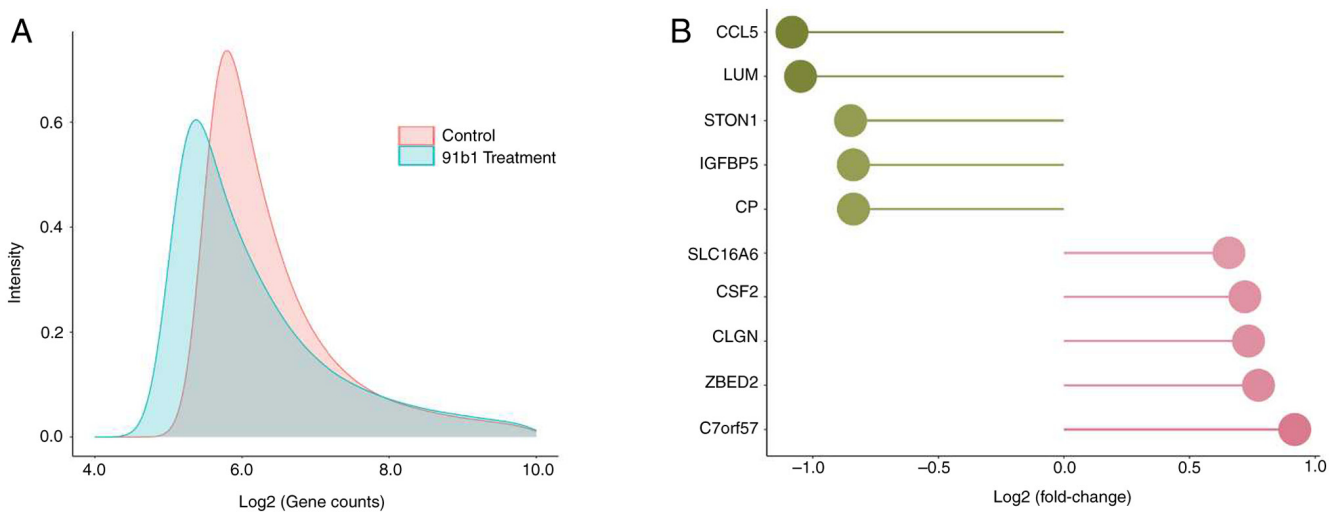

Figure 4. *CCL5* is the gene most downregulated by compound 91b1. (A) Density plots of microarray data of KYSE150 cells treated with compound 91b1 for 48 h vs. blank medium control. (B) the five top genes up- or downregulated by compound 91b1 as identified by microarray analysis. CCL5, chemokine (C-C motif) ligand 5.

Clgn, *Csf2* and *Slc16a6* (Table I and Fig. 4B). *Ccl5* was found to be downregulated in 91b1-treated KYSE150 cells with the highest fold change (-2.12 times), thus 91b1 was a promising anti-cancer compound to inhibit metastasis by targeting *Ccl5*.

The effect of 91b1 on mRNA expression and protein expression of CCL5 in ESCC cells were examined by qPCR analysis and ELISA. All the tested ESCC cell lines showed the reduction in CCL5 mRNA (Fig. 5A-D) and protein expression (Fig. 5E-H) after the treatment with 91b1, which is in agreement with the microarray results using KYSE150. In general, the suppressing effect of 91b1 on CCL5 expression was dose dependent. The results thus confirmed that CCL5 is one of the affected downstream candidates for the cytotoxicity induced by 91b1. The suppression effect of 91b1 on CCL5 protein expression was also demonstrated by IHC staining with CCL5 antibody on KYSE150 cells. The number of cells with cytoplasmic staining signals revealed the relative protein expression level of CCL5. Dark-brownish stained cells in the vehicle-control revealed the high CCL5 protein expression (Fig. 5I) with quantitative analysis (Fig. 5J). Fewer CCL5 positive cells were evident after being treated with increasing concentration of 91b1 for 48 h, suggesting that the protein expression of CCL5 was reduced with 91b1 treatment in a dose-dependent manner.

In vitro cytotoxicity assay of compound 91b1. The anticancer effect of 91b1 on the four ESCC cell lines (KYSE30, KYSE150, KYSE450 and HKESC-4) and two non-tumor cell lines (NE-3 and 293) was evaluated using MTS cytotoxicity assay using CDDP as the positive control (Fig. 6). The MTS_{50} values (concentration of tested compounds that had 50% inhibition on

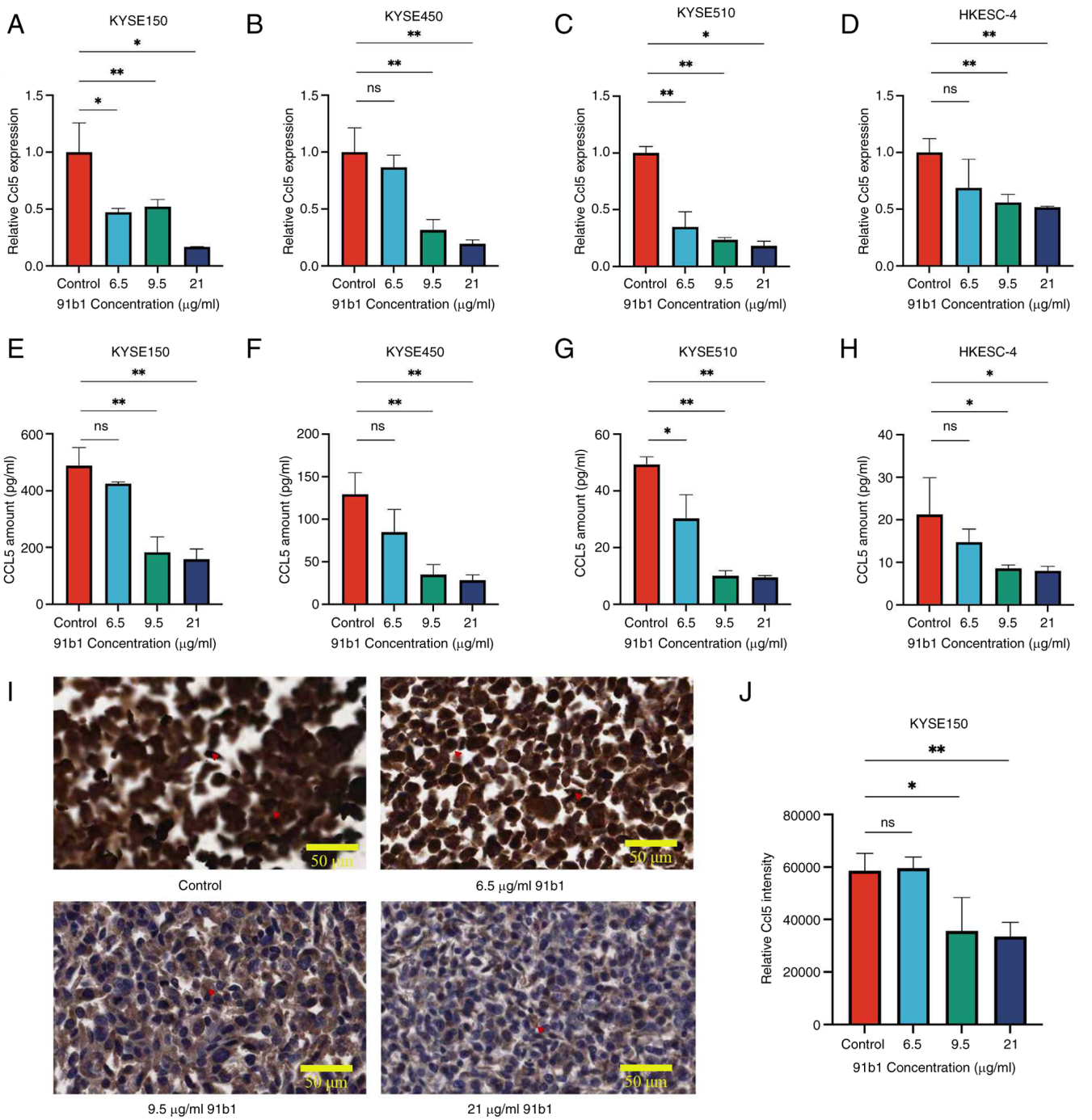

Figure 5. Compound 91b1 downregulates the expression of CCL5 in ESCC cell lines. *CCL5* mRNA expression levels in ESCC cell lines (A) KYSE150, (B) KYSE450, (C) KYSE510 and (D) HKESC-4 after 48-h treatment of 91b1 in different concentrations. Each test was performed in triplicate and relative *CCL5* expression levels were determined by comparing with cells treated with vehicle DMSO (0.05%) following normalized with the expression of β-actin. CCL5 protein expression of (E) KYSE150, (F) KYSE450, (G) KYSE510 and (H) HKESC-4 after 48-h treatment of 91b1 in different concentrations vs. vehicle. Each assay was performed in triplicate. (I) Immunohistochemical staining of CCL5 for KYSE150 treated with vehicle control (DMSO), 6.5, 9.5 and 21 μg/ml 91b1 for 48 h; original magnification, x400; (J) The staining signals were quantitatively analyzed by ImageJ (National Institutes of Health). *P<0.05; **P<0.01; ns, not significant. CCL5, chemokine (C-C motif) ligand 5; ESCC, esophageal squamous cell carcinoma.

MTS activity; Table II). 91b1 showed stronger cytotoxic effect in ESCC cell lines and lesser cytotoxic effect in non-neoplastic cells (NE-3 and 293) than CDDP.

Discussion

Quinoline derivatives have frequently demonstrated anti-cancer properties in previous studies (19,20,39). In the current study, a novel quinoline derivative 91b1 was prepared from the naturally occurring core structure of the 8-hydroxyquinoline. The anticancer effect of 91b1 on esophageal cancer and its effect on the gene expression profile of esophageal cancer cells were evaluated to assess its potential to be explored as a novel anticancer agent.

The present study confirmed by MTS cytotoxicity assay that cytotoxic effects of 91b1 on the five ESCC cells (KYSE30,

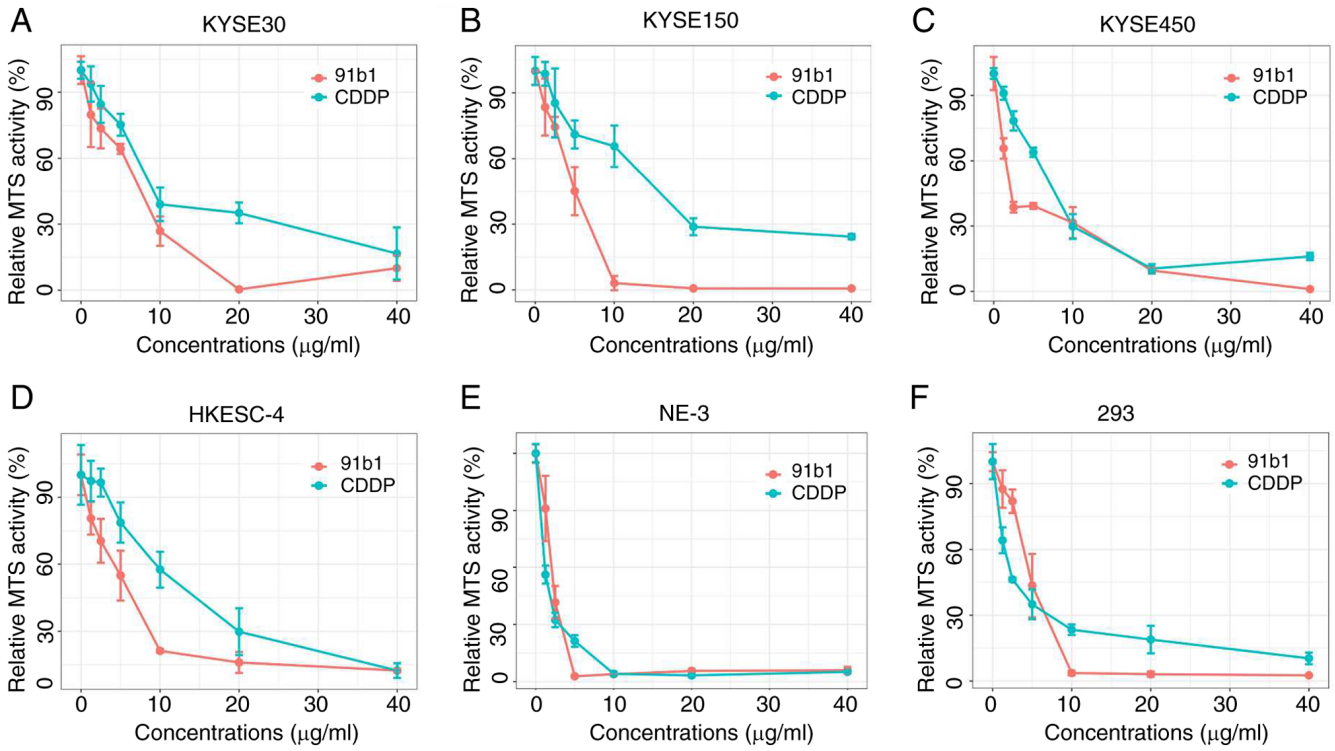

Figure 6. Compound 91b1 shows stronger cytotoxic effect in ESCC cell lines and less cytotoxic effect in non-neoplastic cells. Cytotoxic effects of 91b1 on ESCC cell lines (A) KYSE30, (B) KYSE150, (C) KYSE450, and (D) HKESC-4; and non-neoplastic cell lines (E) NE-3 and (F) 293 were examined by MTS cytotoxicity assay with CDDP as the positive control. Each test was performed in triplicate. ESCC, esophageal squamous cell carcinoma; MTS, [3-(4,5-dimethylthiazol-2-yl)-5-(3-carboxymethoxyphenyl)-2-(4-sulfophenyl)-2H-tetrazolium]; CDDP, cisplatin.

Table II. MTS_{50} (μg/ml) of 91b1 and CDDP for four ESCC cell lines and two non-tumor cell lines. Results were expressed with mean ± SD from triplicate. experiments.

	MTS_{50}	
Cell lines	91b1 (μg/ml)	CDDP (μg/ml)
KYSE30	6.50±0.41	8.00±1.08
KYSE150	4.55±0.77	13.16±2.54
KYSE450	1.80±0.23	6.69±0.34
HKESC-4	4.75±1.83	11.88±1.52
NE-3	1.94±0.29	1.18±0.21
293	4.55±0.87	2.19±0.25

MTS, [3-(4,5-dimethylthiazol-2-yl)-5-(3-carboxymethoxyphenyl)-2-(4-sulfophenyl)-2H-tetrazolium]; CDDP, cisplatin; ESCC, esophageal squamous cell carcinoma.

KYSE150, KYSE450, KYSE510 and HKESC-4) were comparable to that of the first-line chemotherapeutic drug CDDP. CDDP is a well-known chemotherapeutic drug to treat non-small cell lung cancer, ESCC and gastrointestinal cancer (40-42), which was applied as the positive control to assess the anti-cancer potential of compound 91b1. In addition, 91b1 demonstrated less cytotoxicity to non-neoplastic cell lines (NE-3 and 293) than CDDP by 1.6 and 2.1 times respectively. Hence, the current results provided the first evidence about the anticancer potential of 91b1 with lesser cytotoxicity induced on non-tumor cells.

Among the five ESCC cell lines tested, KYSE150 showed sensitivity to CDDP treatment (MTS_{50}; 13.16 μg/ml) but responded positively to the novel quinoline derivative 91b1 (MTS_{50}; 4.55 μg/ml). Subsequent cDNA microarray analysis of KYSE150 identified *Ccl5* as the most downregulated in 91b1-treated KYSE150 cells. *Ccl5*, also known as Human Regulated on Activation in Normal secreted T-cell Expression and Secreted, is one of the members in CC-chemokine family. It is also a well-known chemokine to stimulate tumor progression (5). It mediates its biological effect by activating G protein-coupled receptors CCR1, CCR3 and CCR5 with CCR5 as the dominant receptor (43). The most important role for the interaction between CCL5 and its receptor CCR5 in tumor development is the regulation of metastasis process. The mechanism of metastasis mediated by elevated level of CCL5 remains to be elucidated. However, studies have demonstrated the influence of the CCL5/CCR5 activity on invasion. Secretion of CCL5 by stromal cells in bone marrow was found to enhance the invasion ability of hepatocellular carcinoma cells (44-46).

In the present study, qPCR analysis, ELISA and immunostaining collectively demonstrated the dose-dependent suppression of CCL5 induced by of 91b1, suggesting the anticancer effect is strongly related to the expression of CCL5. Notably, for the expression status of CCL5 in ESCC, 87.5% (7/8) of ESCC cell lines were found to overexpress compared with non-neoplastic esophageal epithelial cells, as revealed by immunostaining. The elevated expression of CCL5 was also observed in ESCC specimens by immunohistochemistry with 76.9% of ESCC tissues showed high expression level for

CCL5. It has been reported that CCL5 may be involved in the early stage of carcinogenesis of ESCC, playing the role in transformation of pre-invasive lesions to cancer as reported in oral squamous cell carcinoma (45). Future investigations could be conducted to elaborate the roles of CCL5 overexpression in pre-malignant lesions of ESCC and other cancers.

Previous reports demonstrate the role of CCL5 in tumor progression including increased invasive abilities (44,46). The ability of CCL5 to enhance the invasion of ESCC cells was further examined by Transwell Matrigel invasion assay, reinforcing its role in tumor progression. Notably, CCL5 (50-500 ng/ml) induced the invasion ability of KYSE30 in the Transwell Matrigel invasion assay, implying that CCL5 can enhance the invasion ability of ESCC cells. To strengthen the association of CCL5 treatment and cell invasion, more experiments, including knock down *Ccl5* by siRNA in a series of ESCC cells, will be performed in the future studies. From the present study, CCL5 expression in the tumor cells can be suppressed by 91b1 and the inhibition of tumor progression based on the suppression of CCL5 expression has been postulated (5). Thus, the overall findings illustrated, for the first time to the best of the authors' knowledge, the potential of 91b1 in suppressing the invasion and progression of ESCC cells through CCL5 suppression.

Some previous studies also suggest that different organs or tissues may secrete different chemokines (including CCL5) along with specific types of lectins and integrins. These molecules facilitate the adhesion of cancer cells to organs, potentially leading to metastasis (47,48). This suggests that the overexpression of CCL5 in other tissues may also increase the risk of tumor metastasis. According to the results of the present study, 91b1 can suppress the expression of CCL5 which may also involve the suppression of metastasis of ESCC cells to other tissue sites. Further studies should explore the anti-metastatic effects of 91b1 on a large across different cancer types.

The present study demonstrated that a novel 8-hydroxyquinoline derivative (5,7-dibromo-1,2,3,4-tetrahydro-2-methylquinolin-8-ol; 91b1) showed a cytotoxic effect on ESCC cells with relatively lower cytotoxicity to non-tumor cells compared with CDDP. 91b1 induced the suppression of mRNA and protein expression of the most downregulated target *Ccl5* in ESCC cells in the dose-dependent manner. CCL5 also enhanced invasive ability of ESCC cells *in vitro* and was found frequently upregulated in ESCC cell lines and tumor tissues. Considering the critical function of CCL5 in cancer development and metastasis, the strategy of suppressing the expression of CCL5 opens a new path for studies on the possible treatment of ESCC using 91b1 and possibly such an approach can be extended to other types of cancer in future. By contrast, the application of quinoline compound is limited by its solubility, retention time, or multi-drug resistance. With the development of novel biological materials, integrating this compound with innovative biomaterials presents a viable pathway to enhance its therapeutic potential and applicability in anti-cancer therapy. Nanomaterials can be employed as carriers to enhance solubility and bioavailability, or designed with specific function for tumor cells to reduce systemic side effects (49). Hydrogels can act as scaffolds due to its biocompatibility and controlled degradation rates for sustained drug delivery (50). Loading 91b1 within hydrogel might offer controlled release for maintaining therapeutic concentrations of drug in tumor or tumor microenvironment over extended period. These strategies aim to address the challenges associated with the clinical application of novel small molecule anticancer drugs such as 91b1 with the unique properties of advanced biomaterials.

The novel quinoline compound 91b1 demonstrated promising anticancer effect to ESCC cells compared with CDDP through the downregulation of CCL5 expression with suppression of tumor invasion. CCL5 was found frequently upregulated in ESCC cell lines and tumor tissues, indicating the high potential use of compound 91b1 for the treatment of ESCC in future. Furthermore, in the present study, while *in vitro* data provide valuable insights, they do not always predict *in vivo* behavior due to the complexity of living organisms. Hence, subsequent *in vivo* studies are crucial for confirming the present findings and understanding the biological relevance of the gene functions studied in ESCC or other types of cancers. Future research should focus on expanding the scope of animal experiments to include mechanism such as related signaling pathway, long-term studies and the evaluation of potential side effects, which will enhance the translational potential of our findings into clinical applications.

Acknowledgements

Not applicable.

Funding

The present study was supported by the research fund of Guangzhou Huashang College (grant no. 2024HSDS09) and the Research in Chirosciences and Chemical Biology (grant no. 1-BBX8) offered by the Hong Kong Polytechnic University It was also supported by the Innovative Technology Commission (HKSAR Government), which established the State Key Laboratory of Chemical Biology and Drug Discovery at Hong Kong Polytechnic University (grant no. ZE20). The present study was also supported by an MOU signed by Hong Kong Baptist University and Griffith University in Australia.

Availability of data and materials

The data generated in the present study may be requested from the corresponding author. All the sequencing data have been deposited in the NCBI GEO depository and are accessible under accession number GEO: GSE273055; https://www.ncbi.nlm.nih.gov/geo/query/acc.cgi?acc=GSE273055.

Authors' contributions

JT, DC, and YZ participated in study design and drafted the article. DC and ZY collected samples, performed the experiments and carried out the initial analysis. PC, YL, KL, and AL performed the further analysis. SL, WH and AC participated in study design. JT and DC confirm the authenticity of all raw data. All authors read and approved the final manuscript.

Ethics approval and consent to participate

Paraffin-embedded specimens containing 26 cancer tissues and 15 non-neoplastic tissues were collected after esophagectomy, with the consent of patients, at the Department of Surgery, Queen Mary Hospital, Hong Kong between January 1990 and December 2001 and the ethics approval for working on the specimens was obtained from the Hong Kong Polytechnic University (approval no. HSEARS20171213007).

Patient consent for publication

Not applicable.

Competing interests

The authors declare that they have no competing interests.

References

1. Then EO, Lopez M, Saleem S, Gayam V, Sunkara T, Culliford A and Gaduputi V: Esophageal cancer: An updated surveillance epidemiology and end results database analysis. World J Oncol 11: 55-64, 2020.
2. Sung H, Ferlay J, Siegel RL, Laversanne M, Soerjomataram I, Jemal A and Bray F: Global cancer statistics 2020: GLOBOCAN estimates of incidence and mortality worldwide for 36 cancers in 185 countries. CA Cancer J Clin 71: 209-249, 2021.
3. Tong D and Law S: Hong Kong experience. In: Ando N (ed). Esophageal Squamous Cell Carcinoma. Springer, Tokyo, pp261-278, 2015.
4. Chan D, Zhou Y, Chui CH, Lam KH, Law S, Chan AS, Li X, Lam AK and Tang JCO: Expression of insulin-like growth factor binding protein-5 (IGFBP5) reverses cisplatin-resistance in esophageal carcinoma. Cells 7: 143, 2018.
5. Aldinucci D, Borghese C and Casagrande N: The CCL5/CCR5 axis in cancer progression. Cancers (Basel) 12: 1765, 2020.
6. Schall TJ, Bacon K, Toy KJ and Goeddel DV: Selective attraction of monocytes and T lymphocytes of the memory phenotype by cytokine RANTES. Nature 347: 669-671, 1990.
7. Brett E, Duscher D, Pagani A, Daigeler A, Kolbenschlag J and Hahn M: Naming the barriers between Anti-CCR5 therapy, breast cancer and its microenvironment. Int J Mol Sci 23: 14159, 2022.
8. Ding H, Zhao L, Dai S, Li L, Wang F and Shan B: CCL5 secreted by tumor associated macrophages may be a new target in treatment of gastric cancer. Biomed Pharmacother 77: 142-149, 2016.
9. Zhang XF, Zhang XL, Wang YJ, Fang Y, Li ML, Liu XY, Luo HY and Tian Y: The regulatory network of the chemokine CCL5 in colorectal cancer. Ann Med 55: 2205168, 2023.
10. Xu H, Zhao J, Li J, Zhu Z, Cui Z, Liu R, Lu R, Yao Z and Xu Q: Cancer associated fibroblast-derived CCL5 promotes hepatocellular carcinoma metastasis through activating HIF1α/ZEB1 axis. Cell Death Dis 13: 478, 2022.
11. Huang R, Wang S, Wang N, Zheng Y, Zhou J, Yang B, Wang X, Zhang J, Guo L, Wang S, *et al*: CCL5 derived from tumor-associated macrophages promotes prostate cancer stem cells and metastasis via activating β-catenin/STAT3 signaling. Cell Death Dis 11: 234, 2020.
12. Chen K, Wang Y, Hou Y, Wang Q, Long D, Liu X, Tian X and Yang Y: Single cell RNA-seq reveals the CCL5/SDC1 receptor-ligand interaction between T cells and tumor cells in pancreatic cancer. Cancer Lett 545: 215834, 2022.
13. Michael JP: Quinoline, quinazoline and acridone alkaloids. Nat Prod Rep 15: 595-606, 1998.
14. Balaraman K, Vieira NC, Moussa F, Vacus J, Cojean S, Pomel S, Bories C, Figadère B, Kesavan V and Loiseau PM: In vitro and in vivo antileishmanial properties of a 2-n-propylquinoline hydroxypropyl β-cyclodextrin formulation and pharmacoki-netics via intravenous route. Biomed Pharmacother 76: 127-133, 2015.
15. Vivanco JM, Bais HP, Stermitz FR, Thelen GC and Callaway RM: Biogeographical variation in community response to root allelochemistry: Novel weapons and exotic invasion. Ecol Lett 7: 285-292, 2004.
16. Huang XQ, Wu RC, Liang JM, Zhou Z, Qin QP and Liang H: Anticancer activity of 8-hydroxyquinoline-triphenylphosphine rhodium(III) complexes targeting mitophagy pathways. Eur J Med Chem 272: 116478, 2024.
17. Prajapati AK, Bhattacharya A and Choudhary S: Inhibiting the activity of malarial drug target Plasmepsin V by quinolines in aqueous medium. J Mol Liq 397: 124158, 2024.
18. Joaquim AR, Gionbelli MP, Gosmann G, Fuentefria AM, Lopes MS and Fernandes de Andrade S: Novel antimicrobial 8-hydroxyquinoline-based agents: Current development, structure-activity relationships, and perspectives. J Med Chem 64: 16349-16379, 2021.
19. Chan SH, Chui CH, Chan SW, Kok SH, Chan D, Tsoi MY, Leung PH, Lam AK, Chan AS, Lam KH and Tang JC: Synthesis of 8-hydroxyquinoline derivatives as novel antitumor agents. ACS Med Chem Lett 4: 170-174, 2012.
20. Lam KH, Lee KK, Gambari R, Kok SH, Kok TW, Chan AS, Bian ZX, Wong WY, Wong RS, Lau FY, *et al*: Anti-tumour and pharmacokinetics study of 2-Formyl-8-hydroxy-quinolinium chloride as *Galipea longiflora* alkaloid analogue. Phytomedicine 21: 877-882, 2014.
21. Lam KH, Lee KK, Kok SH, Wong RS, Lau FY, Cheng GY, Wong WY, Tong SW, Chan KW, Chan RY, *et al*: Antiangiogenic activity of 2-formyl-8-hydroxy-quinolinium chloride. Biomed Pharmacother 80: 145-150, 2016.
22. Pun IH, Chan D, Chan SH, Chung PY, Zhou YY, Law S, Lam AK, Chui CH, Chan AS, Lam KH and Tang JC: Anti-cancer Effects of a Novel Quinoline Derivative 83b1 on human esophageal squamous cell carcinoma through down-regulation of COX-2 mRNA and PGE_2. Cancer Res Treat 49: 219-229, 2017.
23. Lam KH, Lee KK, Gambari R, Wong RS, Cheng GY, Tong SW, Chan KW, Lau FY, Lai PB, Wong WY, *et al*: Preparation of Galipea officinalis Hancock type tetrahydroquinoline alkaloid analogues as anti-tumour agents. Phytomedicine 20: 166-171, 2013.
24. Chan ASC, Tang JCO, Lam KH, Chui CH, Kok SHL, Chan SH, Cheung F, Chor RG and Cheng H: Method of making and administering quinoline derivatives as anti-cancer agents. The Hong Kong Polytechnic University, 2016.
25. Tang JCO, Chan ASC, Lam KH and Chan SH: Quinoline derivatives as anti-cancer agents. Hong Kong Polytechnic University, 2016.
26. Chung PY, Lam PL, Zhou YY, Gasparello J, Finotti A, Chilin A, Marzaro G, Gambari R, Bian ZX, Kwok WM, *et al*: Targeting DNA binding for NF-κB as an anticancer approach in hepatocellular carcinoma. Cells 7: 177, 2018.
27. Zhou Y, Zhou Z, Chan D, Chung PY, Wang Y, Chan ASC, Law S, Lam KH and Tang JCO: The Anticancer effect of a novel quinoline derivative 91b1 through downregulation of *Lumican*. Int J Mol Sci 23: 13181, 2022.
28. Li T, Fu J, Zeng Z, Cohen D, Li J, Chen Q, Li B and Liu XS: TIMER2.0 for analysis of tumor-infiltrating immune cells. Nucleic Acids Res 48 (W1): W509-W514, 2020.
29. Wu T, Hu E, Xu S, Chen M, Guo P, Dai Z, Feng T, Zhou L, Tang W, Zhan L, *et al*: clusterProfiler 4.0: A universal enrichment tool for interpreting omics data. Innovation (Camb) 2: 100141, 2021.
30. Szklarczyk D, Gable AL, Nastou KC, Lyon D, Kirsch R, Pyysalo S, Doncheva NT, Legeay M, Fang T, Bork P, *et al*: The STRING database in 2021: Customizable protein-protein networks, and functional characterization of user-uploaded gene/measurement sets. Nucleic Acids Res 49 (D1): D605-D612, 2021.
31. Shannon P, Markiel A, Ozier O, Baliga NS, Wang JT, Ramage D, Amin N, Schwikowski B and Ideker T: Cytoscape: A software environment for integrated models of biomolecular interaction networks. Genome Res 13: 2498-2504, 2003.
32. Shimada Y, Imamura M, Wagata T, Yamaguchi N and Tobe T: Characterization of 21 newly established esophageal cancer cell lines. Cancer 69: 277-284, 1992.
33. Tang JC, Wan TS, Wong N, Pang E, Lam KY, Law SY, Chow LM, Ma ES, Chan LC, Wong J and Srivastava G: Establishment and characterization of a new xenograft-derived human esophageal squamous cell carcinoma cell line SLMT-1 of Chinese origin. Cancer Genet Cytogenet 124: 36-41, 2001.
34. Cheung LC, Tang JC, Lee PY, Hu L, Guan XY, Tang WK, Srivastava G, Wong J, Luk JM and Law S: Establishment and characterization of a new xenograft-derived human esophageal squamous cell carcinoma cell line HKESC-4 of Chinese origin. Cancer Genet Cytogenet 178: 17-25, 2007.
35. Zhang H, Jin Y, Chen X, Jin C, Law S, Tsao SW and Kwong YL: Cytogenetic aberrations in immortalization of esophageal epithelial cells. Cancer Genet Cytogenet 165: 25-35, 2006.

36. Graham FL, Smiley J, Russell WC and Nairn R: Characteristics of a human cell line transformed by DNA from human adenovirus type 5. J Gen Virol 36: 59-74, 1997.
37. Schmittgen TD and Livak KJ: Analyzing real-time PCR data by the comparative C(T) method. Nat Protoc 3: 1101-1108, 2008.
38. Zhou C, Liu S, Zhou X, Xue L, Quan L, Lu N, Zhang G, Bai J, Wang Y, Liu Z, *et al*: Overexpression of human pituitary tumor transforming gene (hPTTG), is regulated by beta-catenin/TCF pathway in human esophageal squamous cell carcinoma. Int J Cancer 113: 891-898, 2005.
39. Kumar S, Bawa S and Gupta H: Biological activities of quinoline derivatives. Mini Rev Med Chem 9: 1648-1654, 2009.
40. Li S, Shen XY, Ouyang T, Qu Y, Luo T and Wang HQ: Synergistic anticancer effect of combined crocetin and cisplatin on KYSE-150 cells via p53/p21 pathway. Cancer Cell Int 17: 98, 2017.
41. Cesna V, Sukovas A, Jasukaitiene A, Naginiene R, Barauskas G, Dambrauskas Z, Paskauskas S and Gulbinas A: Narrow line between benefit and harm: Additivity of hyperthermia to cisplatin cytotoxicity in different gastrointestinal cancer cells. World J Gastroenterol 24: 1072-1083, 2018.
42. Kryczka J, Kryczka J, Czarnecka-Chrebelska KH and Brzeziańska-Lasota E: Molecular mechanisms of chemoresistance induced by cisplatin in NSCLC cancer therapy. Int J Mol Sci 22: 8885, 2021.
43. Martin L, Blanpain C, Garnier P, Wittamer V, Parmentier M and Vita C: Structural and functional analysis of the RANTES-glycosaminoglycans interactions. Biochemistry 40: 6303-6318, 2001.
44. Singh SK, Mishra MK, Rivers BM, Gordetsky JB, Bae S and Singh R: Biological and clinical significance of the CCR5/CCL5 axis in hepatocellular carcinoma. Cancers (Basel) 12: 883, 2020.
45. Chen D, Yang K, Mei J, Zhang G, Lv X and Xiang L: Screening the pathogenic genes and pathways related to DMBA (7,12-dimethylbenz[a]anthracene)-induced transformation of hamster oral mucosa from precancerous lesions to squamous cell carcinoma. Oncol Lett 2: 637-642, 2011.
46. González-Arriagada WA, Coletta RD, Lozano-Burgos C, García C, Maripillán J, Alcayaga-Miranda F, Godínez-Pacheco B, Oyarce-Pezoa S, Martínez-Flores R and García IE: CR5/CCL5 axis is linked to a poor outcome, and inhibition reduces metastasis in oral squamous cell carcinoma. J Cancer Res Clin Oncol 149: 17335-17346, 2023.
47. Karmakar S and Mukherjee R: Integrin receptors and ECM proteins involved in preferential adhesion of colon carcinoma cells to lung cells. Cancer Lett 196: 217-227, 2003.
48. Langley RR and Fidler IJ: The seed and soil hypothesis revisited-the role of tumor-stroma interactions in metastasis to different organs. Int J Cancer 128: 2527-2535, 2011.
49. Wang C, Zhou H, Kurboniyon MS, Tang Y, Cai Z, Ning S, Zhang L and Liang X: Chemodynamic PtMn nanocubes for effective photothermal ROS storm a key anti-tumor therapy in-vivo. Int J Nanomedicine 19: 5045-5056, 2024.
50. Bordbar-Khiabani A and Gasik M: Smart hydrogels for advanced drug delivery systems. Int J Mol Sci 23: 3665, 2022.